

Polymerization of propylene in a minireactor: Effect of polymerization conditions on particle morphology

Mehrsa Emami, Mahmoud Parvazinia*, Hossein Abedini

Iran Polymer and Petrochemical Institute, P.O.Box 14185/458, Tehran, Iran

Received: 16 October 2017, Accepted: 3 January 2018

ABSTRACT

Gas phase polymerization of propylene was carried out in a semi-batch minireactor using a commercially supported Ziegler–Natta (ZN) catalyst. The influence of variables including monomer partial pressure, external electron donor, reaction temperature and time on the particle morphology and size distribution was investigated. Generally, more uniform fragmentation and particle densities were obtained at lower reaction rates. Monomer partial pressure showed a significant role of particle size and its distribution, the higher the monomer partial pressure, the broader particle size distribution was obtained. Polymerization pressure had a significant role on the morphology of particles. Wider cracks and more porosity were resulted from the polymerizations at higher pressures. Furthermore, a broader particle size distribution was obtained from the polymerizations at higher pressures. The particle size analysis revealed the monomer partial pressure as the most effective parameter on the distribution of particles. The SEM images showed that three different steps could be distinguished in the development of particle morphology within the particle, showing the initiation and development of cracks and appearance of fragments inside the particle. **Polyolefins J (2018) 5: 111-123**

Keywords: Propylene polymerization; gas phase; mini-reactor; Ziegler-Natta; particle morphology.

INTRODUCTION

In heterogeneous polymerization of olefins with supported catalysts, the reaction takes place in the polymer particles formed. Hence, the single particle can be considered as microreactor characterized by its own kinetics and balances of mass and energy [1]. The reagents must be transported from the bulk phase to the particle surface, and from the particle surface to the active cen-

tres of the catalyst. The heat of reaction released at the active sites of the catalyst must be transported through the polymer particle to the particle surface, and afterward to the bulk phase. Fragmentation is critical to provide accessibility of the active centres during polymerization and to allow the particles to expand [2,3,4]. The particle diameter increases from catalyst particle of 20 microns to polymer particle of 1 mm diameter and more [2]. The shape and morphology of a polymer particle

* Corresponding Author - E-mail: M.Parvazinia@ippi.ac.ir

are determined by the shape and initial morphology of the original catalyst and the way the catalyst particle breaks up. For each reactor system, the morphology of the polymer particle is the decisive factor to determine the mass and heat transport [5,6]. Good control of particle morphology to obtain spherical shape, narrow particle size distribution, controlled pore structure, is of great importance to get a good control of micro and macrostructure of the final polymer [2,6,7]. Hence, many efforts have been made to get a balance between high catalyst activity and controlled polymer particle morphology [8-10]. Many models have been developed to get a better understanding of the particle growth and evolution of its morphology [11-13]. It is shown that the accuracy of the model predictions depends on a number of morphological characteristics of particles as well as physical properties of the polymer matrix. Accordingly, it is crucial to have reliable data from the early stages of the reaction when rapid changes of particle properties occur [2,10].

Before utilization of specialty designed reactors, experiments were performed at usual autoclave size reactors to obtain data from initial stages of polymerization [14-16]. Due to the high catalyst productivity, polymerizations had to conduct at very mild conditions, high dilution of monomer, or very short pulses of reactants. These conditions imposed a number of disadvantages: the reaction conditions of these works were far from those used in industry, the exact reaction time was difficult to determine because the quenching or catalyst process was not immediate, also slowing down the reaction rate might change fragmentation and morphology evolution [17,18].

microreactors were applied in the polyolefin field in 1996 to study polymerization of butadiene at low pressure through on-line particle size monitoring [19]. Further developments of the technique enabled studies of the polymerization of other monomers and kinetic studies at the relevant industrial conditions (temperatures up to 70°C and pressures up to 35 bar) [20-22]. Good control over flow rate, mixing, reactor pressure, residence time, mass and heat transfer which results in enhanced reproducibility, are of advantages of the use of micro-reactor devices [23].

The best approach to study the initial stages of olefin polymerization to follow heterogeneous catalyst frag-

mentation, particle growth and polymerization kinetics, is to use well-defined reactor conditions with off-line analysis of the product [24]. In this way, specially designed stopped-flow reactors are developed by researchers. The Short-Stop gas phase, is a successful example of these reactors. In this technique, gas phase polymerizations are carried out continuously in a fixed packed bed reactor. This experimental set-up had potential of performing the polymerization similar to that performed in industrial conditions [25,26]. This research was developed by calorimetric method to follow heat transfer, polymerization kinetics and evolution of catalyst temperature during the first seconds of reaction [27-28]. Cancelas studied heat transfer and overheating of particles with the aim of using this reactor to determine optimum catalyst injection conditions to the gas-phase reactors [29]. One of the methods introduced for morphological and kinetic studies is quenched-flow in which slurry polymerizations are carried out for a defined time inside a mixing element, and then stopped by feeding the reaction media into a quenching vessel [30-32].

An experimental set-up capable of obtaining reliable data on the kinetics, and evolution of particle morphology and polymer properties during the very early stages of the catalytic olefin polymerization is not introduced heretofore. Each of mentioned techniques has advantages and disadvantages. For instance, on-line techniques are difficult to use in realistic industrial conditions. In slurry stopped-flow techniques, the morphology will be influenced by the phase of the reaction. In gas phase stopped-flow technique (short stop reactor), there is a fundamental difference between the heat transfer in the fixed bed reactor and continuous, full-scale fluidized bed reactors.

In this work, a gas phase mini-reactor experimental setup is developed. Propylene polymerization at constant pressure with monomer injection at the precision of 0.01 bar is enabled. The influence of process variables including monomer partial pressure, reaction temperature and also external electron donor on the final particle morphology (surface morphology, size and size distribution) is investigated. The obtained experimental data will be helpful to support modelling works especially on the fragmentation behaviour during the initial moment of the reaction.

EXPERIMENTAL

Chemicals

Fourth generation of Ziegler-Natta catalyst (industrial grade) supported on $MgCl_2$ with 2.4 wt% of Mg was utilized. Polymerization grade propylene (99.99%), triethyl aluminum (TEAL) and cyclohexyl methyl dimethoxy silane (electron donor type C) and dicyclopentyl dimethoxy silane (electron donor type D) were provided by Maroun Petrochemical Co., Mahshahr. Also, distilled n-hexane (polymerization grade by Pars Cylinder Co., Isfahan, Iran) dried overnight in the presence of sodium wire and molecular sieves, was used as the solvent.

Polymerization

Polymerization set-up

Gas-phase reactions were carried out in a house-made mini-reactor. The reactor (Figure 1) was a stainless steel cylinder with a diameter of 6 mm and a depth of 25 mm. The reactor was equipped with two solenoid valves controlled by a logic controller equipped with home-made software for the feed. The reactor pressure was monitored with a pressure transmitter. The feed gas line (propylene) was purified with three commercial purifiers. The feeding gas was pre-heated while passing through the heating unit, as shown in Figure 1. The heating unit was a long coil inserted in a heating bath, with 4 meters length of the tube to ensure that the gas temperature reaches the desired tem-

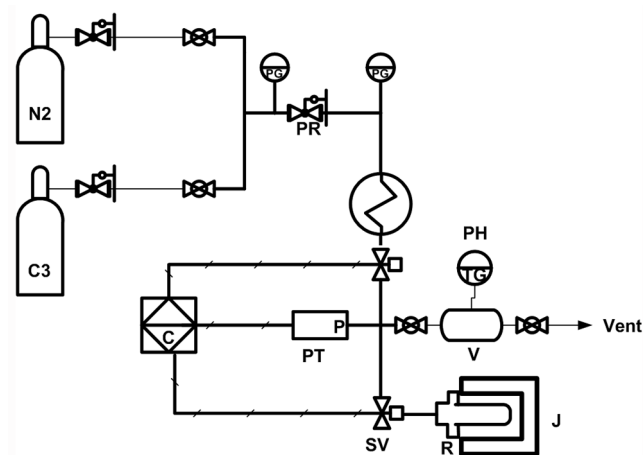


Figure 1. Polymerization set-up with mini-reactor, C3: monomer, N_2 : inert gas, PG: pressure gauge, PH: gas pre-heat, PR: pressure regulator, R: mini-reactor, J: jacket, PT: pressure transmitter, V: storage vessel.

perature. A heating bath was used to maintain the temperature of the reaction medium at the desired value. A K-type thermocouple was used to monitor the inlet gas temperature. The reactor was filled with pre-activated catalyst in a glove box to avoid contamination of the contents, and then fixed to the gas line. The reactor was then plunged into a heat jacket (connected to heating bath) to ensure constant reaction temperature during the reaction. Pressure and temperature of monomer feed were controlled. Polymerizations at different temperatures and pressures with commercial Ziegler-Natta catalyst were enabled using the explained mini-reactor. Monomer consumption evaluation at high precisions (0.01 bar), from the beginning of polymerization was enabled. The rate of reaction was calculated during polymerization using instance monomer consumption.

Polymerization procedure and reproducibility

Pre-activated, dried 4th generation of Ziegler-Natta catalyst was used in all experiments. A small amount of the catalyst (about 5 mg) was weighed into the reactor and the reactor was enclosed in the glove box. The reactor was brought out of the glove box and connected to the propylene line in mini-reactor setup. Polymerizations with different conditions were carried out using the same activated batch of the catalyst. The polymerization time ranged from 1s to 2h. The polymerization temperature range was 40-70°C and the monomer pressure was 2-10bar. Overall polymer yield was measured by weighing the catalyst used and final polymer samples. Also, for each monomer injection pulse, time interval and pressure changes were measured and individual catalyst productivity was calculated. Therefore, a graph of the rate of polymerization versus time was plotted. It is clear that an optimization of the reaction conditions was necessary to avoid catalyst deactivation or even particle coagulation due to local polymer melting. To ensure that the results were reproducible, polymerization kinetics was examined by performing two experiments with the same procedure and recipe (runs NC6-1,2 and NC63,4 in Table 1). Figure 2 shows the rate profile obtained from similar polymerizations at different reaction times. As can be seen in Figure 2, rate profiles match well each other.

Table 1. Reaction conditions used in the experiments.

Run	Catalyst (mg)	Temp. (°C)	N ₂ (bar)	Total pressure (bar)	Time (min)	Product (mg)	Yield (g _{por} /g _{cat})	Particle mean diameter(μ)
NC4-1	1.3	70	1	8	12	126.8	57.5	215
NC4-3	1.7	50	1	8	12	68.4	40	180
NC4-4	3.3	40	1	8	12.5	100.3	50.5	210
NC4-5	3	40	1	4	12	8.4	2.5	109
NC4-6	3.5	40	1	6	12	38.2	10.9	134
NC5-1	5.5	70	1	2	12	22.1	4.0	119
NC5-2	4.2	70	1	6	12	83.2	19.8	181
NC5-3	4.5	70	1	4	12	76.8	17.0	201
NC5-4	3.1	70	1	8	12	80.5	26.0	166
NC6-1	4	70	1	8	7	86.7	21.7	175
NC6-2	5.2	70	1	8	3	60.1	11.6	131
NC7-6	3.9	60	1	8	7	53.7	13.8	152
NC7-5	5.8	60	2	8	7	38	6.55	108
G3*	2	70	1	8	12	84.1	84.15	187

*External electron donor: Cyclohexyl methyl dimethoxysilane (CMMS-C Donor).

Characterization

Particle size measurement

To measure the size of particles, a thin layer of particles was spread on a microscope lam. Images of about 400 particles were taken with the aim of microscope. Each particle was sized individually, and then mean particle size was calculated for each sample.

SEM imaging

Morphology of final polymer particles was observed with scanning electron microscopy (SEM). Particle morphology images were recorded using a VEGA microscope (SEM) (TESCAN, Czech Republic) operating at accelerating voltages of 10 or 15 keV (depending on each individual case). As the catalyst used (and especially its morphology) was highly sensitive to moisture, it was essential to carry out SEM observations under inert conditions.

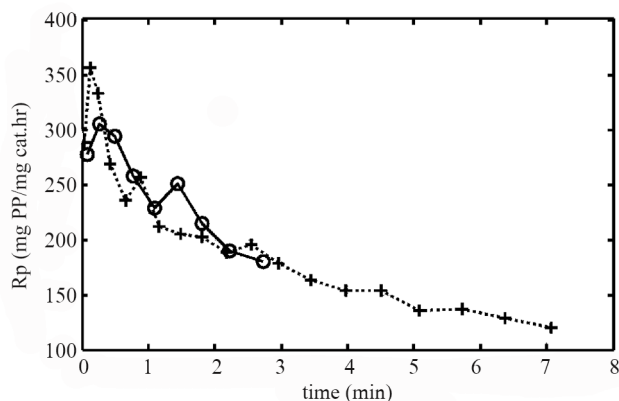


Figure 2. Rate profile for two experiments carried out in gas phase at different times, reactor pressure: 6 bar, temp.: 70°C time (7 min :+, 3 min:○).

RESULTS AND DISCUSSION

The objective of this work was to investigate the process variables that affect particle morphology (surface morphology, size and size distribution) at relatively low reaction yields. As mentioned earlier, good control of particle morphology to obtain spherical shape, narrow particle size distribution, controlled pore structure, is of great importance to get a good control of micro and macrostructure of the final polymer [2,6,7]

Morphology studies

Effect of different variables was examined on the morphology of particles. Some parameters showed a considerable effect on the morphology, while some others, at least in the range of applied variations in the experiments, were less effective.

Effect of polymerization temperature

To study the effect of polymerization temperature on the particles morphology, three different experiments were carried out at 8 bar pressure and different temperatures (runs NC4-1,3,4 in table1). SEM images of particles obtained from different polymerization temperatures are shown in Figure 3. Figure 3 shows that the reaction temperature exerts significant influence on the particles morphology, increases the temperature from 40 to 70°C, leads to formation of cracks on the surface of the catalyst/polymer particles, and increases the porosity of particles. Also as Figure 3 shows, when the polymerization temperature reduced,

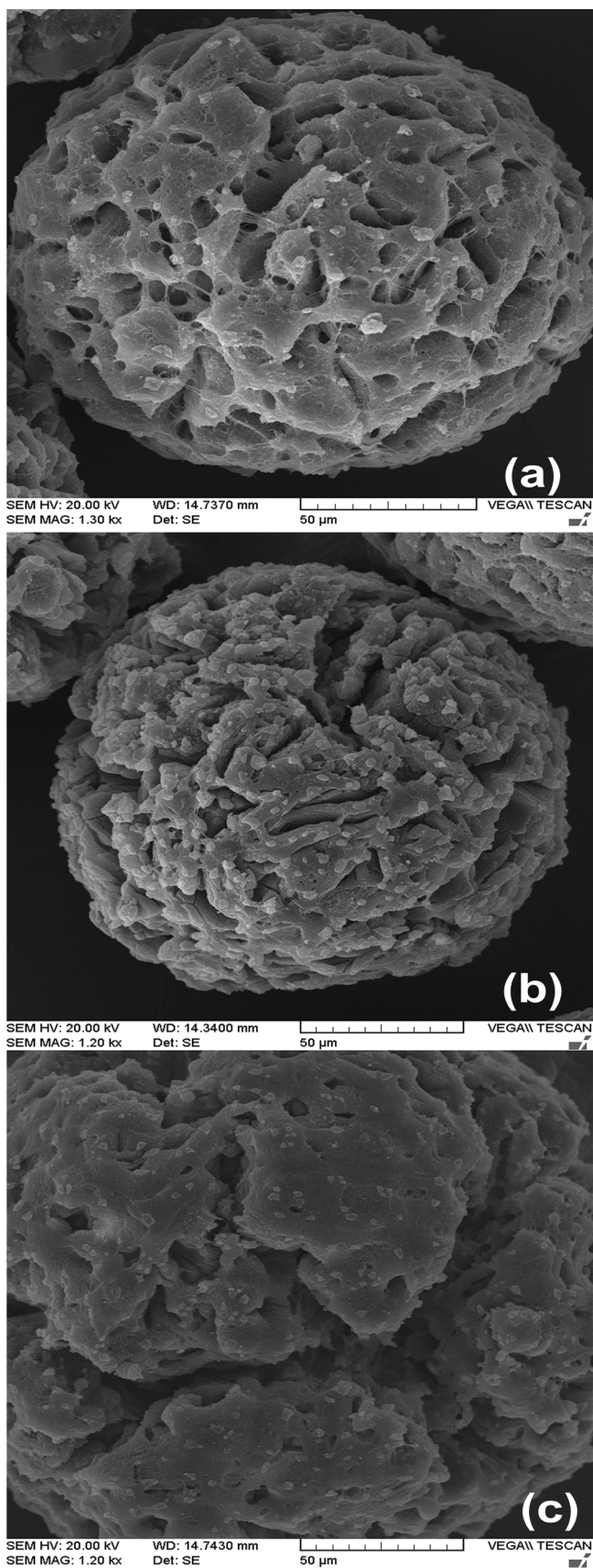


Figure 3. Scanning electron micrographs of surface of single particles obtained from gas phase polymerization at different temperatures. reactor pressure: 8 bar, time: 12 min, and reaction temp. (a): 70°C, (b): 50°C, (c):40°C.

the catalyst fragments became smaller with more uniform distribution; Figure 3(b) clearly shows better distribution of catalyst fragments.

Pater et.al. carried out catalytic polymerization of propylene at low reaction rates in slurry phase. They observed a dense polymer skin around large clusters, each of them consisting of a large number of micro particles at low polymerization rates. They showed, at high polymerization temperatures, the skin disappeared, leading to an open macro-porous structure accompanied by a fast decrease of the polymer bulk density [16].

Studies of Silva et.al obtained from the continuous gas-phase after 2s, showed that the morphology of polyethylene particles were strongly dependent on the temperature. They explained that the presence of large cracks was related to the insufficient energy dissipation of the particles at higher temperatures [25]. Particle size distributions of particles obtained from polymerizations at different temperatures are showed in Figure 4. As can be seen in Figure 4, at the polymerization conditions we imposed, polymerization temperature slightly affects particle size distribution. By increasing temperature, reaction rate increases which results in larger particles.

Kiparissides et.al. developed a mathematical model to predict the evolution of particle size distribution (PSD) in a gas-phase olefin polymerization fluidized bed reactor (FBR). According to the model, as the bulk phase temperature increases, the PSD becomes broader while its mean value is shifted towards larger particle sizes. They explained it by the increasing po-

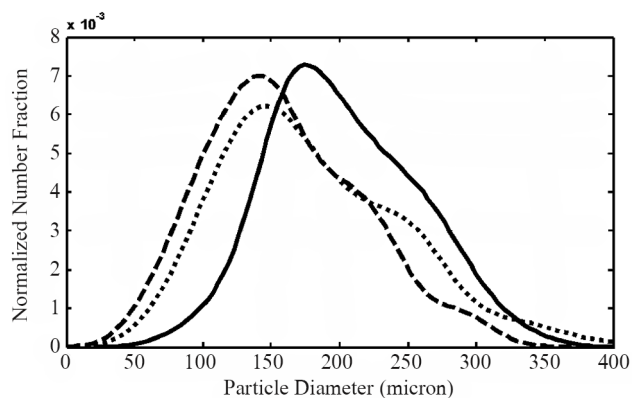


Figure 4. Particle size distribution of particles obtained from polymerizations at different temperatures; total reactor pressure: 8 bar, time: 12 min, and reaction temp.: (....) 50°C, (---) 60°C, (___) 70°C.

lymerization rate at high temperatures and long tails of the PSD obtained at high temperatures related to the agglomeration of particles [33,34].

Effect of monomer partial pressure

Investigation of the effect of monomer partial pressure on particle morphology was carried out by comparing two similar runs at different monomer partial pressures and total reactor pressure of 8 bar and 70°C (runs NC7-5,6 in Table 1). Figure 5 displays the morphology of particles obtained from these experiments. It can be seen from Figures 5(a) and 5(b), with increasing the initial inert pressure from 1 to 2 bar, the catalyst fragments become more uniform. This can be due to better energy dissipation of the particles due to lower reaction rates at decreased monomer partial pressure. Studies of Tioni et.al. in a specially packed-bed stopped flow minireactor, for catalytic reaction of ethylene in gas phase showed the presence of 33% molar helium as inert in the feed was sufficient to avoid thermal runaway for the catalyst they used at 6 bars of monomer and 80°C [27].

Investigations of Pater et.al. showed a first-order dependence of lowering polymerization rate with an inert would not be expected. Actually, a much stronger decrease of the polymerization rate might be found due to enrichment of the inert inside the porous particle [1].

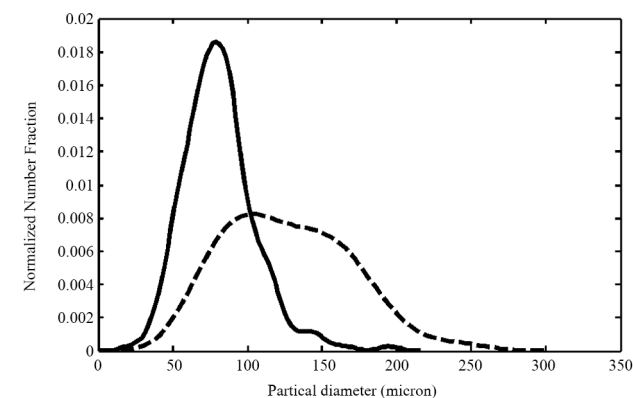
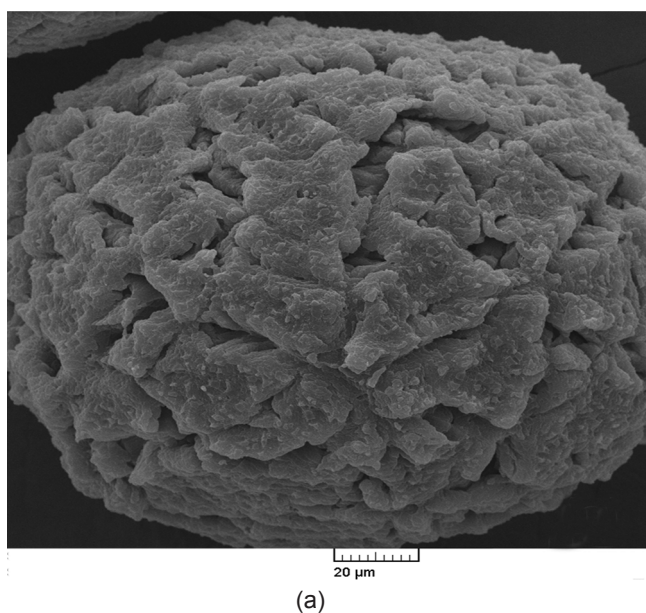


Figure 6. Effect of monomer partial pressure on particle size distribution; line: 6 bar monomer, dotted: 7 bar monomer, total reactor pressure: 8 bar, time: 12 min.

Figure 6 compares the particle size distribution of samples obtained from the polymerizations carried out at 7 and 6 bar partial pressure of monomer. As can be seen in Figure 6, monomer partial pressure plays a significant role on particle size and its distribution. When monomer partial pressure increases from 6 to 7 bar, mean particle size increases from 108 to 152 μ m (Table 1) and size distribution varies significantly and becomes rather broad.

Effect of external electron donor

Effect of external electron donor on particle morphology was studied too. Two runs with different external electron donors of types C and D, at 70°C, 8 bar

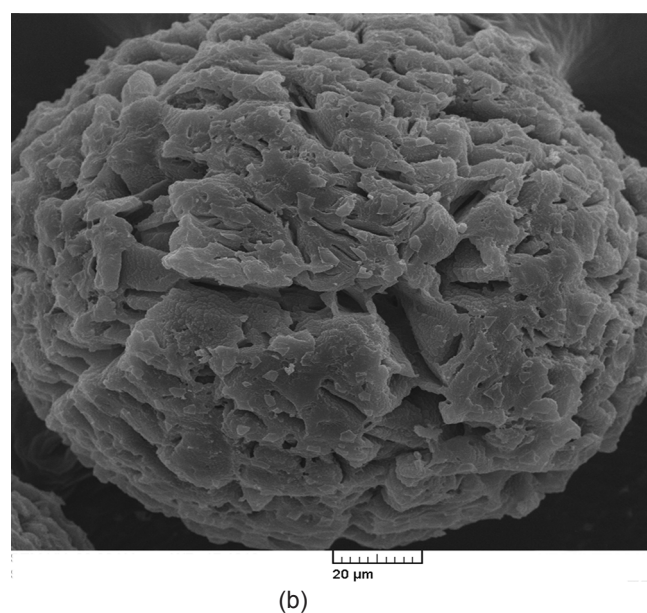
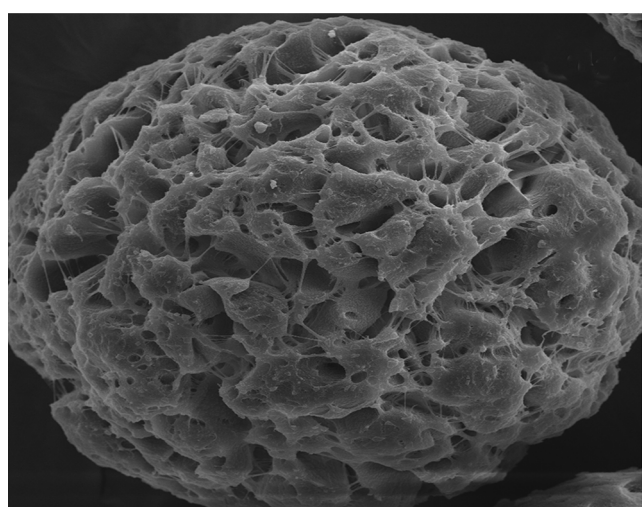
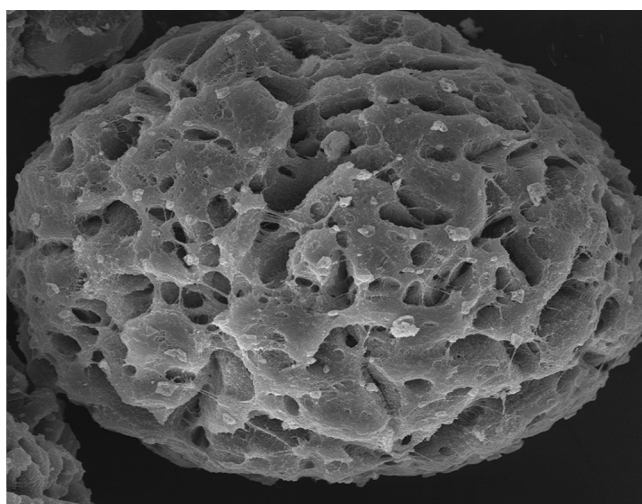


Figure 5. Scanning electron micrographs of surface of single particles obtained from polymerizations at different monomer partial pressures (a): 7 bar monomer, (b): 6 bar monomer total reactor pressure: 8 bar, reaction temp.: 70°C, time: 12 min.

pressure and 12 min were carried out (runs G3 and NC4-1 in Table1). The morphology of particles obtained from these experiments is displayed in Figure 7, which shows surface particle morphology is by the type of external electron donor. However, the results in Table 1 show that the external electron type D increases the productivity of the catalyst. The sizes of particles were also analyzed and compared in Figure 8. The results show, the external electron donor type D shifts the maximum number fraction to the bigger size, though has not changed the distribution of particle sizes significantly.



(a)



(b)

Figure 7. Scanning electron micrographs of surface of single particles obtained from polymerization with different external electron donors; total reactor pressure: 8 bar, reaction temp.: 70°C, time: 12 min (a): C Donor (b): D Donor.

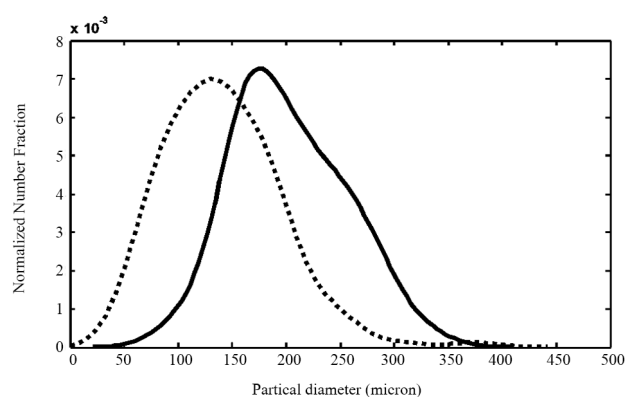


Figure 8. Particle size distribution of particles obtained from polymerizations with different external electron donors; total reactor pressure: 8 bar, reaction temp.: 70°C, time: 12 min line (D Donor) and dotted (C Donor).

Effect of polymerization pressure

In order to investigate the effect of polymerization pressure on final particle size and morphology, experiments were performed at different polymerization pressures. These experiments were performed at two reaction temperatures, 40 and 70°C. Figure 9 shows the morphology of particles obtained from the polymerizations at 70°C and 12 min in the pressure range from 2 to 8 bar (runs NC5 1 to 4 in Table1). As can be seen in Figure 9, at 70°C, by increasing the polymerization pressure from 2 to 8 bar, the polymerization yield increases from 4 to 126.8 mg.mg⁻¹_{cat} h⁻¹. As the pressure increases 4 times, the yield of polymerization

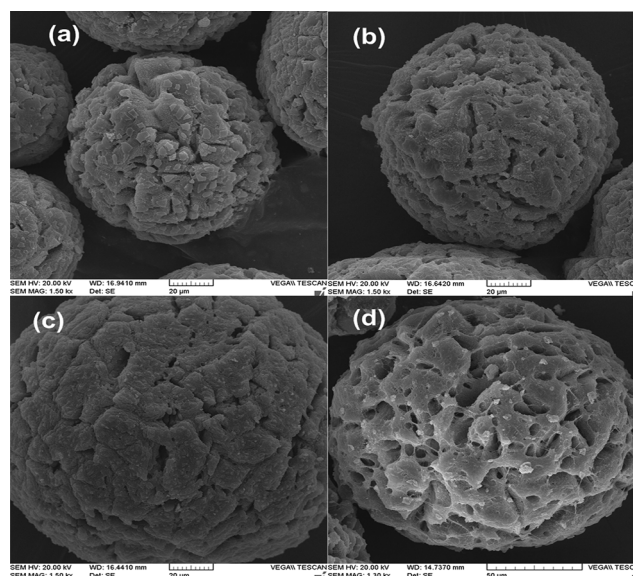


Figure 9. Scanning electron micrographs of surface of single particles obtained from polymerizations at different pressures; reaction temp.: 70°C, time: 12 min total reactor pressure (a): 2 bar, (b): 4 bar, (c): 6 bar, (d): 8 bar.

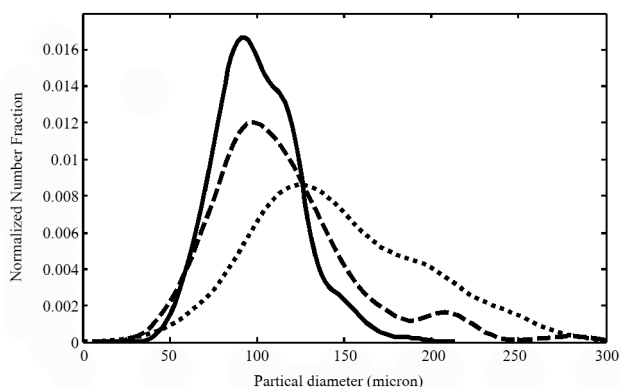


Figure 10. Particle size distribution of particles obtained at 70°C, different polymerization pressures, reaction temp.: 70°C, time: 12 min, total reactor pressure: (—) 2 bar, (---): 4 bar, (....) 6 bar.

increases about 30 times. Figure 9d shows the morphology of particle obtained from the polymerization at 8 bar pressure. The morphology of the particle obtained at 8 bar pressure in comparison those of three other particles is clearly different, and has wider holes and the particle looks less dense. In Figure 10, the particle size distributions of particles obtained from the polymerization at 70°C are compared. The results in Figure 10 show, the polymerization pressure has a significant role on the size and size distribution of particles. With increasing the polymerization pressure, the maximum number fraction of particles shifts to bigger sizes with broader size distribution.

Figure 11 shows the effect of total reaction pressure on particle morphology for the experiments carried out at 40°C, after 12 min (runs NC4-4 to 6 in Table1). It can be seen in Figures 11 a-c that with increasing the polymerization pressure from 2 to 6 bar, cracks are formed in the particle and when the pressure is set to 8 bar, wider cracks are formed. If we consider the formation of cracks as a negative point in replication phenomenon, it can be concluded that in our experiments, optimized reaction conditions are 40°C and 4 bar pressure to access good replication. The sizes of particles obtained from the polymerization at 40°C were also analyzed and compared in Figure 12. The results in Figure 12 show, the polymerization pressure has a significant role on the size and distribution of particle sizes. Particles obtained at 4bar has narrow size distribution with a maximum number fraction at 100μ, but when the polymerization pressure increases

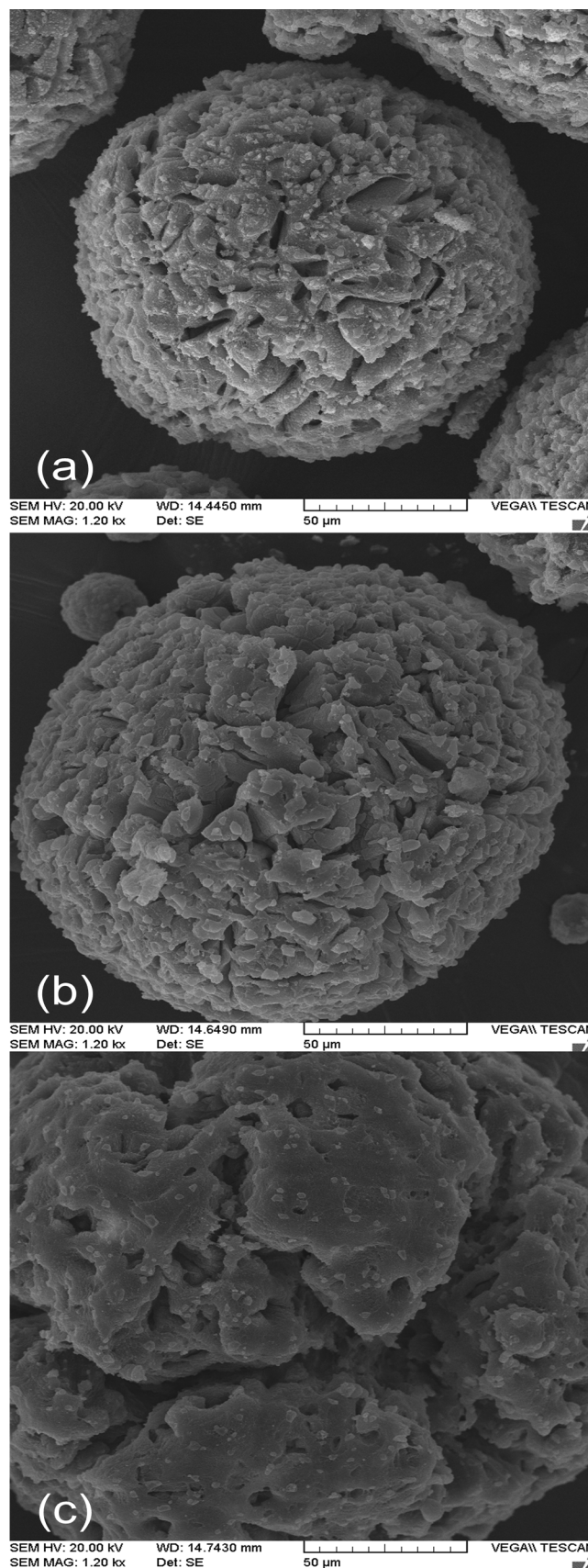


Figure 11. Scanning electron micrographs of surface of single particles obtained from different polymerization pressures; reaction temp.: 40°C, time: 12 min, total reactor pressure (a): 4 bar, (b):6 bar, (c):8 bar.

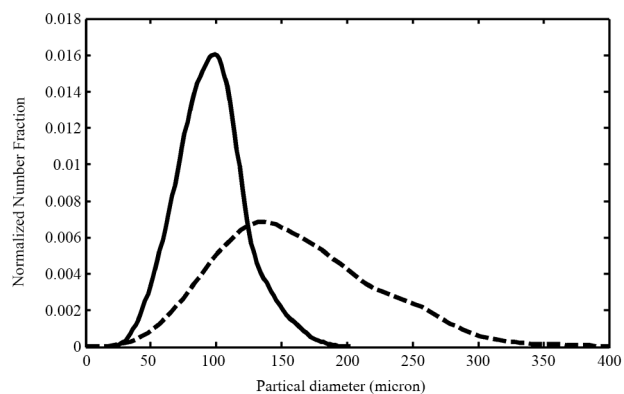


Figure 12. Particle size distribution of particles obtained from polymerization at different pressures. reaction temp.: 40°C, time: 12 min, total reactor pressure; line: 4 bar, dotted: 8 bar.

to 8 bar, the mean particle size increases to 210 μ (see Table 1), but the size distribution becomes very broad. Formation of wide cracks in the particles at 8 bar can be the reason to widen particle size distribution (Figure 11c).

Effect of polymerization time

This series of experiments (NC6-1,2, NC4-1) was intended to explore the effect of the reaction progress on the particle morphology, so a number of experiments performed at similar conditions and stopped at different times. Figure 13 shows the morphology of particles obtained from the polymerizations at 70°C and 8 bar, in different polymerization times. It is obvious in Figure 13 that particle morphology is transformed from a smooth closed surface to a rough porous as the reaction proceeds. Figure 13 clearly shows the development of the particle morphology. In Figure 13a, the particle morphology after 3 min is shown. The cauliflower like morphology of the particle shows disintegration of clusters and onset of crack formation after 3 min. Figure 13b shows the growth of initial cracks and initiation of new cracks. In Figure 13c, the development of subglobules and appearance of wide cracks and holes are obvious. Therefore, three different steps in the development of particle morphology can be distinguished. The first step is initiation of cracks in the particle due to internal particle pressure as reaction proceeds and more polymers are produced inside the particle. In the second step, fragments can be clearly distinguished and cracks get wider as a result of particle growth. In this step, cracks initiate at each fragment.

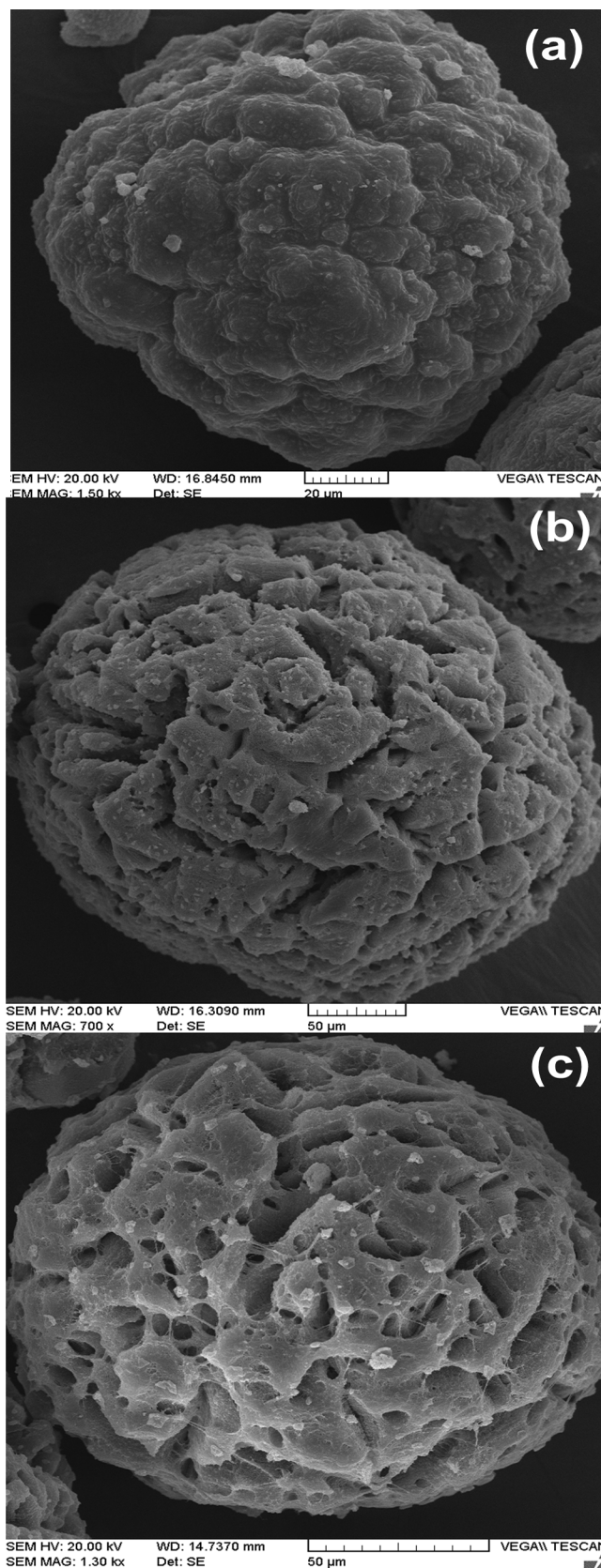


Figure 13. Scanning electron micrographs of surface of single particles obtained from polymerizations at different times; total reactor pressure: 8 bar, reaction temp.: 70°C time: (a): 3 min, yield=11.6mg/mgcat (b):7 min, yield=20.6 mg/mgcat; (c):12 min, yield=57.5 mg/mgcat.

In the third step, each fragment behaves like initial particle and due to fragment growth, cracks get to be wider and they clearly are appeared on the fragments. Experimental studies of Noristi et.al. in propylene polymerization with $MgCl_2$, supported Ziegler-Natta catalyst on samples having different degrees of polymer growth (from 0.1 to 1000 g/g of catalyst) showed that the particle surface, transformed from a smooth appearance to agglomerate of subparticles. However, it must be mentioned that their results related to a polymerization carried out under very mild reaction conditions, in which heat and mass transfer limitations were almost absent [14]. So the question is why by increasing reaction time, segregated fragments are developing and holes and cracks developed in the particle. This phenomenon is explained by a mathematical model describing the single particle growth in heterogeneous polymerization of olefins considering elastic tensions inside growing particles. This model implies that concentration gradients due to mass transfer resistance, increases the probability of particles to rupture and if the particles are internally homogeneous, they will rupture at the centre. This can lead to the formation of porous particles that expand more rapidly than particles without rupture. The catalyst goes through a breakup process after a few seconds of polymerization when the largest tensions arise [35].

The particle size distributions of samples obtained from the polymerization at $70^\circ C$ are compared in Figure 14. Figure 14 and Table 1 show the size of particles increases with polymerization time due to the progress of the reaction. But the size distribution of

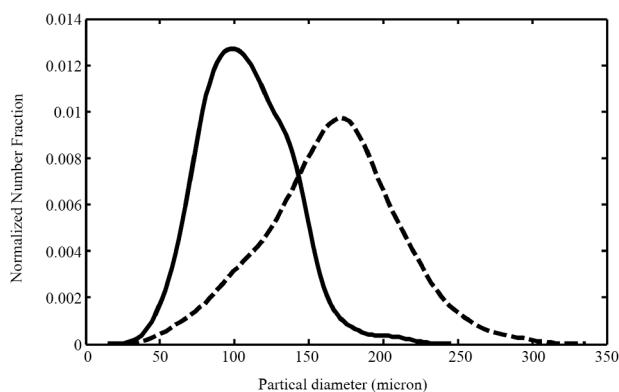


Figure 14. Particle size distribution of particles obtained at different polymerization times; total reactor pressure: 8 bar, reaction temp.: $70^\circ C$ line: 3 min, dotted: 7 min.

particles becomes broader with time. As mentioned above, formation of wide cracks in the particles can be the reason to widen particle size distribution with the reaction progress. Mulhaupt et.al. Studied evolution of PSD during ethylene slurry polymerizations in 2010. Polymer particle growth was monitored online using a Lasentec Focused Beam Reflectance Measurement (FBRM) and Video Microscopy (PVM) Probes. Their experiments were carried out at constant pressure of 3 bar, and evolution of PSD was studied by a prepolymerized morphology-controlled Ziegler catalyst. The results of the online particle growth measurements showed that in the course of the polymerization, the position of maximum number fraction of particles and shape of the PSD did not vary significantly, but the particles diameter increased continuously [36].

CONCLUSION

Semi-batch polymerization of propylene using Ziegler–Natta catalyst in gas phase mini-reactor was carried out. Effects of different parameters, particularly polymerization pressure, temperature and time as well as external electron donor, on the particle morphology (surface morphology, size and size distribution) were evaluated. The SEM images showed, the parameters affecting the reaction rate like monomer partial pressure, external electron donor, and temperature, can directly manipulate the particle morphology. The results showed that with increasing the polymerization temperature from $40^\circ C$ to $70^\circ C$ the holes in the particles were increased by number and size. Also, by reduction of polymerization temperature, the catalyst fragments became smaller with more uniform distribution. At the polymerization conditions we imposed, the polymerization temperature slightly affected the particle size distribution. Monomer partial pressure showed significant role of particle size and its distribution, the higher the monomer partial pressure, the broader particle size distribution was obtained. The results showed that the external electron donor type D increased productivity of the catalyst and shifted the maximum size to the bigger amounts, though it did not change the distribution of particle sizes significantly. The polymerization yield showed non-linear propor-

tion to the polymerization pressure. As pressure increased 4 times, yield of polymerization showed an increase of about 30 times. The polymerization pressure showed significant role of the morphology of particles. Wider cracks and more porosity were resulted from the polymerization at 8bar. Although, the maximum number fractions obtained from 8bar and 6 bar were the same size, the particles obtained from 6 bar showed a narrower size distribution. The results showed, at the polymerization temperature of 40°C, monomer pressure had a significant role on the size and distribution of particles. The particles obtained at 4bar had narrow size distribution and showed good replication of the primary catalyst. Wide holes and cracks formed at 8 bar could be the reason to obtain wider particle size distribution.

Evolution of particle morphology with time was investigated too. As the reaction proceeded, the fragmentation was developed and also the porosity of particles was increased. By increasing the reaction time, the size distribution shifted toward higher diameters, and the distribution became wider. Progressive increasing of particle size with reaction time showed that the reaction was not limited to the surface of particle. The crack formation was related to concentration gradients due to mass transfer resistance, which increased the probability of particle rupture. Three different steps in the development of particle morphology were distinguished. First step: initiation of cracks; second step: appearance of fragments inside the particle; third step: growth of cracks inside the fragments.

ACKNOWLEDGMENTS

The authors would like to specially thank Mr. F.Hormozi for set-up construction assistance. Furthermore, the authors wish to thank Maroun Petrochemical Company, MPC, for supplying catalyst and Mrs. F. Khosravi and L. Tolami for microscopic images.

REFERENCES

1. Weickert G, Meier GB, Pater, JT M, Westerterp KR (1999) The particle as microreactor: Catalytic propylene polymerizations with supported metallocenes and Ziegler–Natta catalysts. *Chem Eng Sci* 54: 3291-3296
2. Severn JR, Chadwick JC Eds. (2008) Tailor-made polymers: via immobilization of alpha-olefin polymerization catalysts. John Wiley & Sons, GMBH, ch. 3, 79-81
3. Pasquini N, Antonio A (2005) Polypropylene handbook. Hanser publisher, Munich, Ch.2, 75-82
4. Martin C, Mc Kenna TF (2002) Particle morphology and transport phenomena in olefin polymerisation. *Chem Eng J* 87: 89-99
5. Cecchin G, Marchetti E, Baruzzi G (2001) On the mechanism of polypropene growth over MgCl₂/TiCl₄ catalyst systems. *Macromol Chem Phys* 202:1987-1994
6. Grof Z, Kosek J, Marek M (2005) Modeling of morphogenesis of growing polyolefin particles. *AIChE J* 51: 2048-2067
7. Zheng X, Pimplapure MS, Weickert G, Loos J (2006) Influence of porosity on the fragmentation of Ziegler-Natta catalyst in the early stages of propylene polymerization. *E-Polymers* 6: 356-365
8. Ferrero MA, Chiovetta MG (1991) Effects of catalyst fragmentation during propylene polymerization. IV: Comparison between gas phase and bulk polymerization processes. *Polym Eng Sci* 31: 904-911
9. Pater J, Weickert G, Van Swaaij WP (2003) Polymerization of liquid propylene with a fourth generation Ziegler–Natta catalyst: Influence of temperature, hydrogen, monomer concentration, and prepolymerization method on powder morphology. *J Appl Polym Sci* 87: 1421-1435
10. Horackova B, Grof Z, Kosek J (2007) Dynamics of fragmentation of catalyst carriers in catalytic polymerization of olefins. *Chem Eng Sci* 62: 5264-5270
11. Kittilsen P, Svendsen HF, McKenna TF (2003) Viscoelastic model for particle fragmentation in olefin polymerization. *AIChE J* 49: 1495-1507
12. Kittilsen P, Mc Kenna TF, Svendsen H, Jacobsen HA, Fredriksen SB (2001) The interaction between mass transfer effects and morphology in heterogeneous olefin polymerization. *Chem Eng*

- Sci 56: 4015-4028
13. Najafi M, Parvazinia M, Ghoreishy MHR, Kiparissides C (2014) Development of a 2D single particle model to analyze the effect of initial particle shape and breakage in olefin polymerization. *Macromol React Eng* 8: 29-45
 14. Noristi L, Marchetti E, Baruzzi G, Sgarzi P (1994) Investigation of the particle growth mechanism in propylene polymerization with $MgCl_2$ -supported Ziegler–Natta catalysts. *J Polym Sci* 32: 3047-3059
 15. Zheng X, Loos J (2006) Morphology evolution in the early stages of olefin polymerization. *Macromol Symp* 236: 249-258
 16. Pater JT, Weickert G, Loos J, van Swaaij WP (2001) High precision prepolymerization of propylene at extremely low reaction rates—Kinetics and morphology. *Chem Eng Sci* 56: 4107-4120
 17. Taniike T, Funako T, Terano M (2014) Multilateral characterization for industrial Ziegler–Natta catalysts toward elucidation of structure–performance relationship. *J Cat* 311: 33-40
 18. McKenna TF, Di Martino A, Weickert G, Soares JB (2010) Particle growth during the polymerisation of olefins on supported catalysts, 1–nascent polymer structures. *Macromol React Eng* 4: 40-64
 19. Eberstein C, Garmatter B, Reichert KH, Sylvester G (1996) Gasphasen polymerisation von Butadien. *Chemie Ingenieur Technik* 68: 820-823
 20. Oleshko VP, Crozier PA, Cantrell RD, Westwood AD (2001) In-situ and ex-situ microscopic study of gas phase propylene polymerization over a high activity $TiCl_4$ - $MgCl_2$ heterogeneous Ziegler-Natta catalyst. *Macromol Rapid Commun* 22: 34-40
 21. Pater J, Weickert G, van Swaaij WP (2003) Optical and infrared imaging of growing polyolefin particles. *AIChE J* 49: 450-464
 22. Abboud M, Kallio K, Reichert KH (2004) Video microscopy for fast screening of polymerization catalysts. *Chem Eng Tech* 27: 694-698
 23. Bneke J (2014) Microreactors: A new concept for chemical synthesis and technological feasibility. *Mat Sci Eng* 39: 89-101
 24. Mc Kenna TF, Tioni E, Ranieri MM, Alizadeh A, Boisson C, Monteil V (2013) Catalytic olefin polymerisation at short times: Studies using specially adapted reactors. *Can J Chem Eng* 91: 669-686
 25. Silva FM, Broyer JP, Novat C, Lima EL, Pinto JC, McKenna TF (2005) Investigation of catalyst fragmentation in gas-phase olefin polymerisation: A novel short stop reactor. *Macromol Rapid Commun* 26: 1846-1853
 26. Taniike T, Thang VQ, Binh NT, Hiraoka Y, Uozumi T, Terano M. (2011) Initial particle morphology development in Ziegler-Natta propylene polymerization tracked with stopped-flow technique. *Macromol Chem Phys* 212: 723-729
 27. Tioni E, Spitz R, Broyer JP, Monteil V, McKenna TF (2012) Packed-bed reactor for short time gas phase olefin polymerization: Heat transfer study and reactor optimization. *AIChE J* 58: 256-267
 28. Browning B, Sheibat-Othman N, Pitault I, McKenna TF (2014) A 2-D observer to estimate the reaction rate in a stopped flow fixed bed reactor for gas phase olefin polymerization. *AIChE J* 60: 3511-3523
 29. Cancelas AJ, Monteil V, McKenna TF (2017) Impact of catalyst injection conditions on the gas phase polymerization of propylene. *React Chem Eng* 2: 75-87
 30. Di Martino A, Broyer JP, Spitz R, Weickert G, McKenna TF (2005) A rapid quenched-flow device for the characterisation of the nascent polymerisation of ethylene under industrial conditions. *Macromol Rapid Commun* 26: 215-220
 31. Di Martino A, Weicker G, McKenna TF (2007) Contributions to the experimental investigation of the nascent polymerisation of ethylene on supported catalysts. *Macromol React Eng* 1: 165-184
 32. Di Martino A, Weickert G, McKenna TF (2007). Contributions to the experimental investigation of the nascent polymerisation of ethylene on supported catalysts. *Macromol React Eng* 1: 229-242
 33. Kanellopoulos V, Dompazis, G, Gustafsson B, Kiparissides C (2004) Comprehensive analysis of single-particle growth in heterogeneous olefin polymerization: The random-pore polymeric flow model. *Ind Eng Chem Res* 43: 5166-5180

34. Dompazis G, Kanellopoulos V, Kiparissides C (2005) A multi scale modeling approach for the prediction of molecular and morphological properties in multi site catalyst, olefin polymerization reactors. *Macromol Mat Eng* 290: 525-536
35. Di Martino A, Weickert G, Sidoroff F, McKenna TF (2007) Modelling induced tension in a growing catalyst/polyolefin particle: A multi scale approach for simplified morphology modelling. *Macromol React Eng* 1: 338-352
36. Xalter R, Mülhaupt R (2010) Online monitoring of polyolefin particle growth in catalytic olefin slurry polymerization by means of lasentec focused beam reflectance measurement (FBRM) and video microscopy (PVM) Probes. *Macromol React Eng* 4: 25-39